Dielectric Properties and Conduction Mechanism of Li-Ni-Ferrites

S. M. Attia[a] and T. M. Meaz[b]

[a]Physics Department, Faculty of Science, Kaferelshikh University, Kafer El-Shiekh, Egypt.
[b]Physics Department, Faculty of Science, Tanta University, 31527 Tanta, Egypt.

Polycrystalline samples of the composition $Ni_{1-x}Li_{0.5x}Fe_{2+0.5x}O_4$ (where x=0.0, 0.25, 0.5, and 0.75) were prepared by the standard ceramic method. The dielectric constant, ε', and AC electrical conductivity, σ', were determined at different temperature and frequencies. The values of the dielectric constant are abnormally high and approaches around 10^{11}. The dielectric constant decreases with increase of the frequency. The multiple hopping conduction mechanism is used to explain the conduction mechanism in theses materials. The results show that the conductivity of these materials is very sensitive to the temperature.

1. Introduction

Spinel ferrites have vast application from microwave to radio frequencies; it is of great importance from both the fundamental and the applied research points of view [1.2]. The characteristic physical properties of the spinel ferrites, as electrical conductivity, Dielectric constant, thermoelectric power, magnetic property arises from the ability of these compounds to distribute the cations amongst the available tetrahedral A- and octahedral B-sites [3.4]. The factors related to the ionic charge and radius, crystal and ligand fields, and anion polarization play an important role in the site preference of cation.

Lithium ferrites are very attractive for microwave applications instead of garnets and other spinel ferrites [5]. Mitra et al. [6] had prepared bulk Li substituted Ni–Zn ferrites and obtained ferrites with improved microstructure and magnetic properties. El Nimr *et al.* [7] had prepared nano particles of $Li_{0.1}(Ni_{1-x}Zn_x)_{0.8}Fe_{2.1}O_4$ and studied their particle size distribution, DC conductivity and magnetic permeability. Several studies [8–11] have been reported on the effect of additions of divalent, trivalent and tetravalent ions on the electrical conductivity and dielectric properties of lithium ferrites. P. V. Reddy and T. S. Rao [12] studied the transport properties of Li-Ni mixed

ferrite. They found that the charge carrier concentration and the charge carrier concentration decrease with the temperature. J. Jing, et. al., [13] prepared a series of $LiNi_{0.5}La_xFe_{2-x}O_4$ by thermolysising of oxalate precursors and studied their crystal structure and magnetic properties. The cation distribution of these samples shows that Li ion prefers to occupy the octahedral site. P. G. Kharabe, et. al., [14] prepared a series of $Li_{0.5}Ni_{0.75-x/2}Cd_{x/2}Fe_2O_4$ and studied their crystal structure and magnetic properties as well as their dielectric properties.

In this work we present an investigation on the dielectric properties and the conduction mechanism of $Ni_{1-x}Li_{0.5x}Fe_{2+0.5x}O_4$, where x = 0.0, 0.25, 0.5, and 0.75.

2. Experimental Methods

The samples were prepared by the standard ceramic method [14], where high pure NiO, Fe_2O_3, and Li_2CO_3 were mixed together in a proper ratio in order to prepare a series of $Ni_{1-x}Li_{0.5x}Fe_{2+0.5x}O_4$, where x = 0.0, 0.25, 0.5, and 0.75. After grounding, the mixtures were presintered at 900 °C for 6 hours in porcelain crucibles using an electric muffle furnace, and left to cool to room temperature. The mixtures were ground again for 6 hours to get a fine powder. The powder is, then, pressed in die to get disc-shaped samples of diameter 1.3 cm under pressure 10 bar. The discs are sintered at 1150 °C for 6 hours and left to cool to room temperature. Finally, the samples were polished to obtain two smooth uniform parallel plates surfaces. Contacts on the sample surface were made by silver paste for electrical measurements. The crystal structure of the sample was confirmed to be a single phase cubic spinel using x-ray difrractometer (not shown). AC electrical conductivity and the dielectric properties of each sample were determined by using LCR meter (type- HIOKI 3532-50) in the frequency range 100 Hz –5 MHz and in the temperature range from room temperature up to around 700K.

3. Results and dissections

3.1 Dielectric Properties

The variation of the dielectric constant ε′ with the frequency at different selected temperatures is shown in Fig. (1) as log-log scale for $Ni_{1-x}Li_{0.5x}Fe_{2+0.5x}O_4$. It is shown that the values of the dielectric constant are abnormally high; it is around 10^6 or more at room temperature and approaches 10^{11} at high temperature. The value of the dielectric constant depends on the frequency and temperatures. The behavior of the dielectric constant with the frequency is normal, *i.e.*, ε' decreases with increasing frequency. As the temperature increases, the dielectric constant increases. The results show also that the dielectric constant exhibits a week dependence on the composition.

Same behavior was reported for other ferrites [15]. The behavior of the dielectric constant can be explained on the bases of the relaxation theory in solids. It is well known that the complex dielectric constant ($\varepsilon^* = \varepsilon' + j\varepsilon''$) of the medium vary with the angular frequency ($\omega=2\pi f$) according to the following equation [16].

$$\varepsilon^* = \varepsilon_\infty + \frac{(\varepsilon_o - \varepsilon_\infty)}{(1 + j\omega\tau)} \qquad (1)$$

where τ is the relaxation time, ε_o is the static field dielectric constant, and ε_∞ is the high-frequency (optical) dielectric constant of the material. The real and imaginary parts of the complex dielectric constant ε', ε'' respectively can be expressed as

$$\varepsilon' = \varepsilon_o + \frac{(\varepsilon_o - \varepsilon_\infty)}{(1 + \omega^2\tau^2)} \qquad (2)$$

and

$$\varepsilon'' = (\varepsilon_o - \varepsilon_\infty) + \frac{\omega\tau}{(1 + \omega^2\tau^2)} \qquad (3)$$

Equation (2) gives an explanation to the decrease of the dielectric constant with increasing frequency. From the other hand, the behavior of dielectric constant with the frequency can be explained on the fact that the hopping of the charge carriers can not follow the frequency of the external applied electric field beyond a certain frequency value [17]. ε'' represents the dielectric loss through the material.

Figure (2) depicts the variation of the dielectric constant with the temperature at different selected frequencies (10^2, 10^3, 10^4, 10^5, 10^6, 5×10^6 Hz) for all samples. It is shown that, the dielectric constant, ε', increases with increasing temperature. This behavior may be attributed to the existence of strong correlation between conduction mechanism and dielectric polarization in ferrite [18, 19]. As the temperature increases the number of charge carriers increases, resulting in an enhanced build-up of space charge polarization and hence an increase in the dielectric properties.

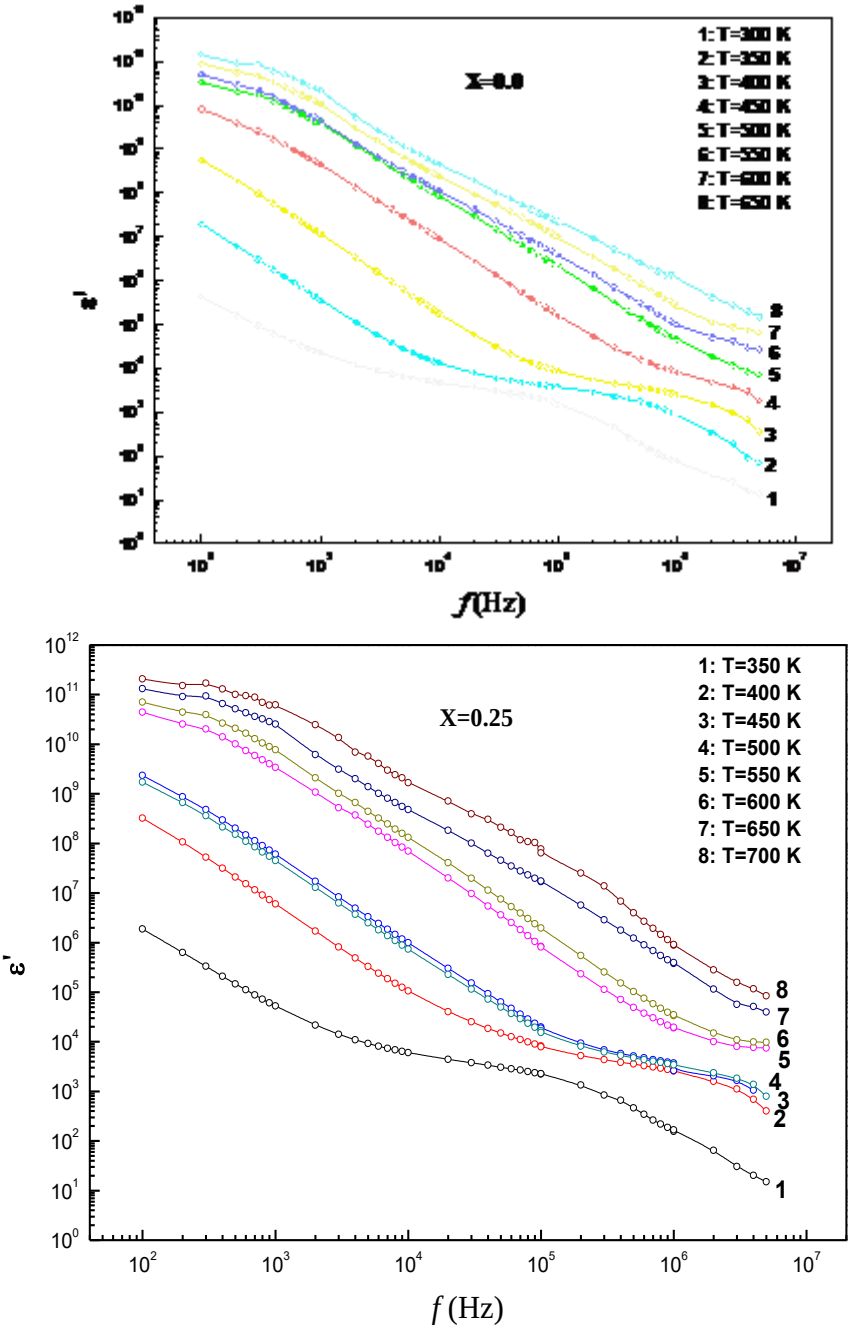

Fig. (1 a:b): The variation of dielectric constant, ε′, with the frequency, *f* (Hz), at different selected temperatures for $Ni_{1-x}Li_{0.5x}Fe_{2+0.5x}O_4$ samples with (x=0.0 & x.=0.25).

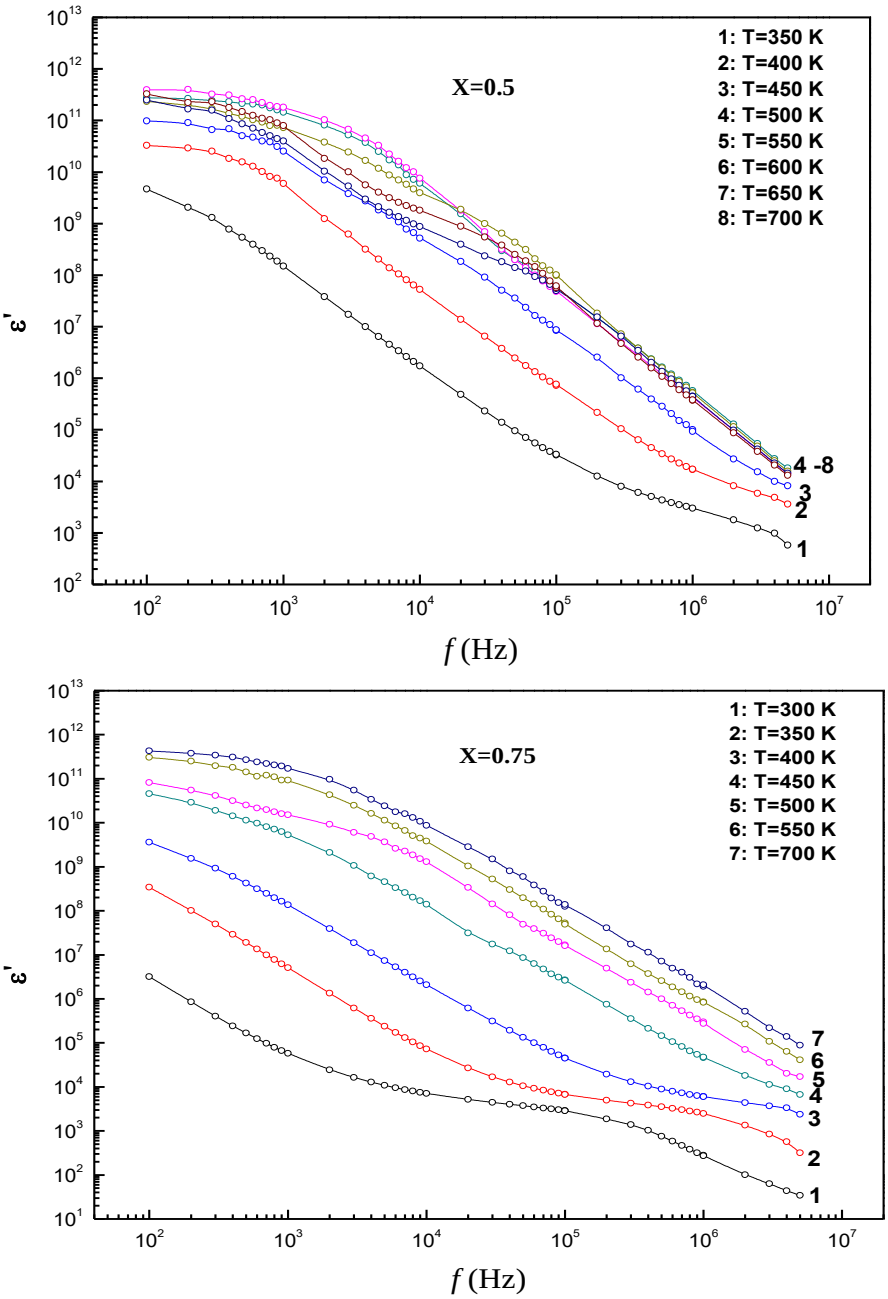

Fig. (1. c:d): The variation of dielectric constant, ε′, with the frequency, *f* (Hz), at different selected temperatures for $Ni_{1-x}Li_{0.5x}Fe_{2+0.5x}O_4$ samples with (x=0.5 & x.=0.75)

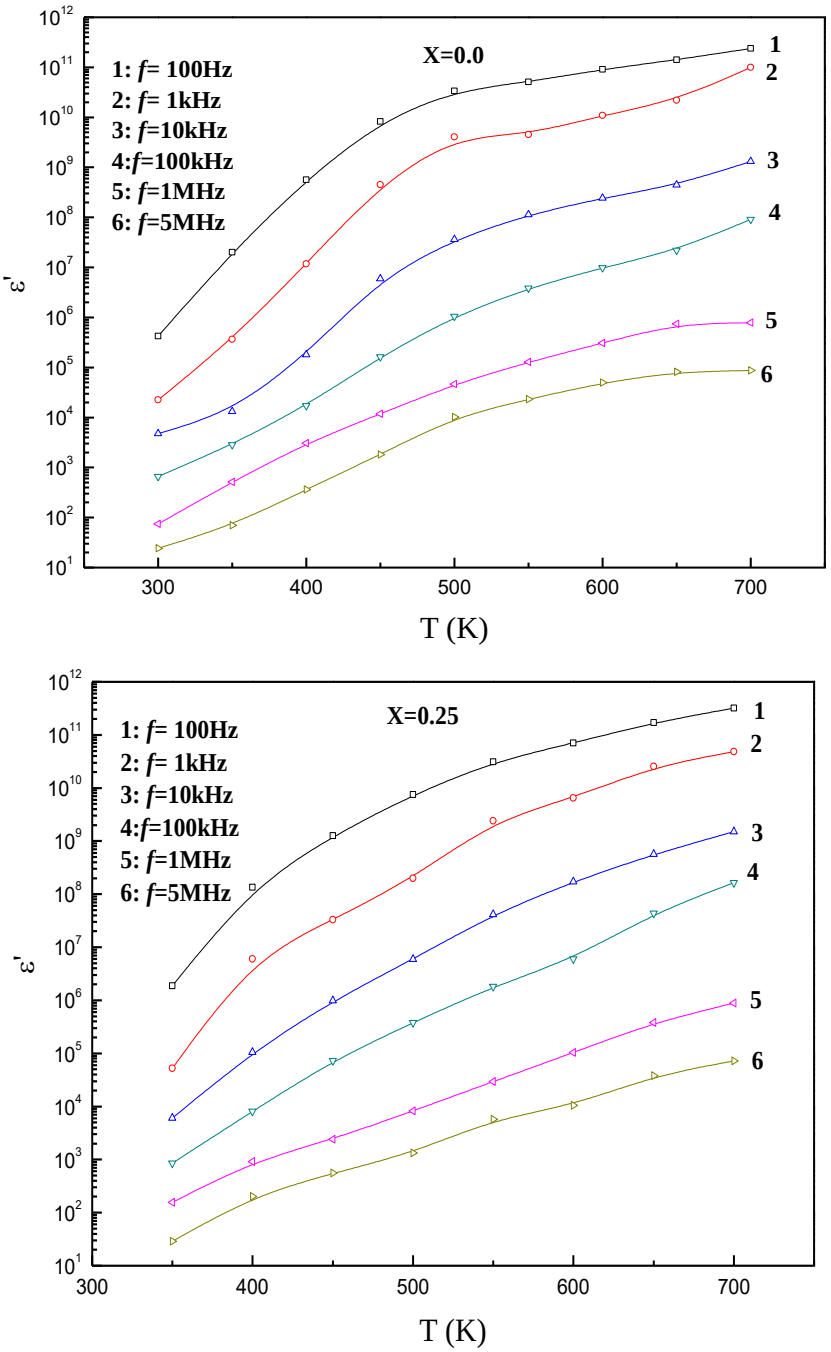

Fig. (2.a : b): The variation of the dielectric constant, ε′, with temperature, T(K), at different selected frequencies for $Ni_{1-x}Li_{0.5x}Fe_{2+0.5x}O_4$ samples with (x=0.0 & x.=0.25).

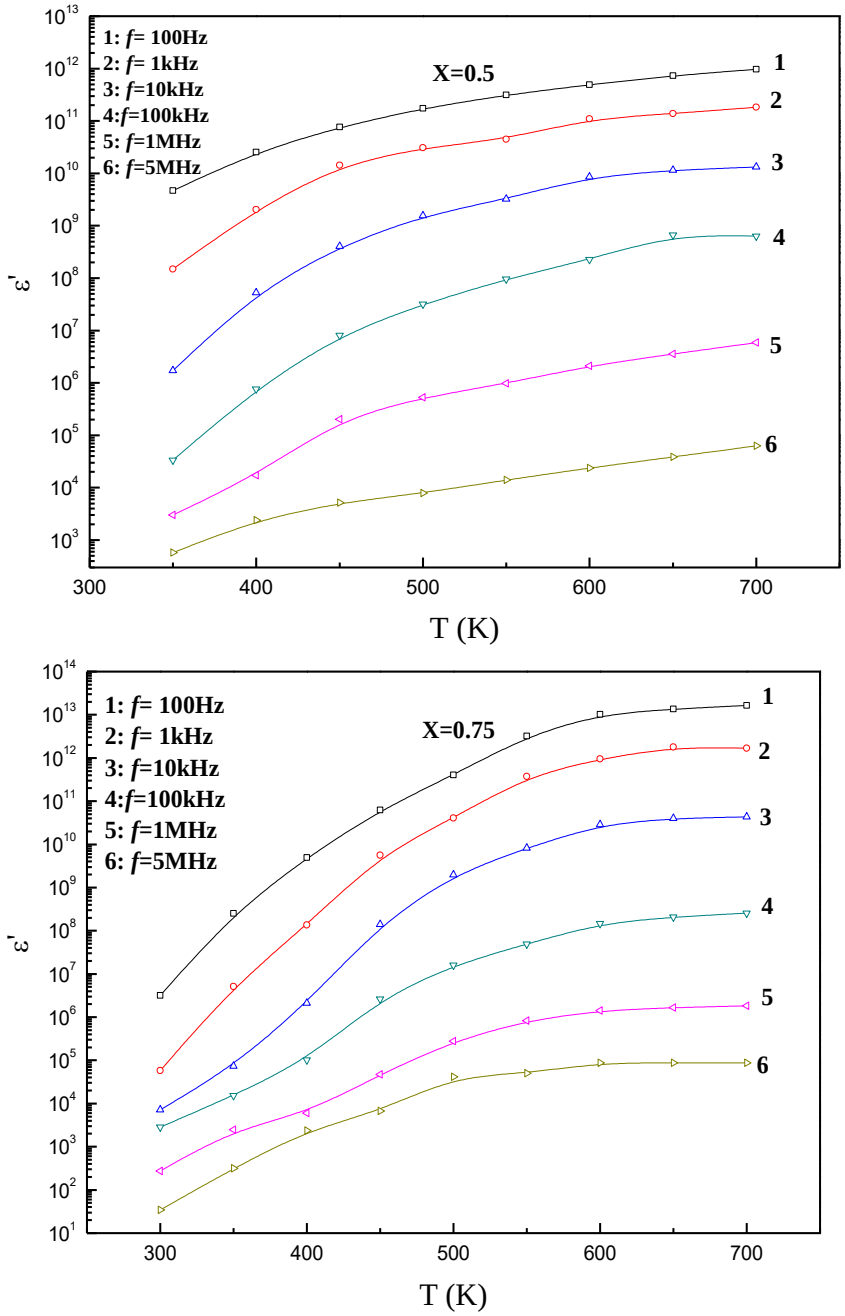

Fig. (2 c : d): The variation of the dielectric constant, ε′, with temperature, T(K), at different selected frequencies for $Ni_{1-x}Li_{0.5x}Fe_{2+0.5x}O_4$ samples with (x=0.5 & x.=0.75)

The dielectric loss tangent, tanδ measures directly the phase difference due to loss of energy within the sample at a particular frequency [20]; tanδ is given by

$$\tan\delta = \frac{\varepsilon''}{\varepsilon'} \qquad (4)$$

Figure (3) illustrates the variation of dielectric loss tangent tanδ with the frequency at different selected temperatures for all prepared samples. It is shown that the dielectric loss tangent exhibits a peaking feature with the frequency, where the peaks are shifted towards higher frequencies with increasing temperature. The peaking behavior of tanδ with the frequency can be explained on the basis of the previous assumption [18, 19] that a strong correlation exists between the conduction mechanism and the dielectric polarization of ferrite. The peaks in tanδ curves are observed when the hopping frequency of charge carriers coincides with that of the external electric field [17]. The shift of the peaks of tanδ to higher frequencies with increasing temperature is due to the increase of the natural hopping frequency of the charge carriers with increasing temperature. In this case.

$$\omega\tau = 2\pi \qquad (5)$$

i.e. $\omega\tau = 1$ turn, where τ is the relaxation time of the hopping process and ω is the angular frequency of the external field ($\omega = 2\pi f_{max}$) [21]. The relaxation time τ can be written as [22]

$$\tau = \tau_o e^{E_D/(kT)} \qquad (6)$$

where τ_o is the relaxation time at infinity high temperature, E_D is the activation energy for dielectric relaxation, and k is Boltzmann constant. Fig. (4) shows the logarithmic representation of the relaxation time τ versus $10^3/T$ for the samples with x =0.0, 0.25, and 0.75. Each sample exhibits a straight line with slope equal to E_D/k. Table (1) lists the values of the dielectric activation energy E_D. The activation energy of the dielectric relaxation E_D lies between 0.36 to 0.47 eV.

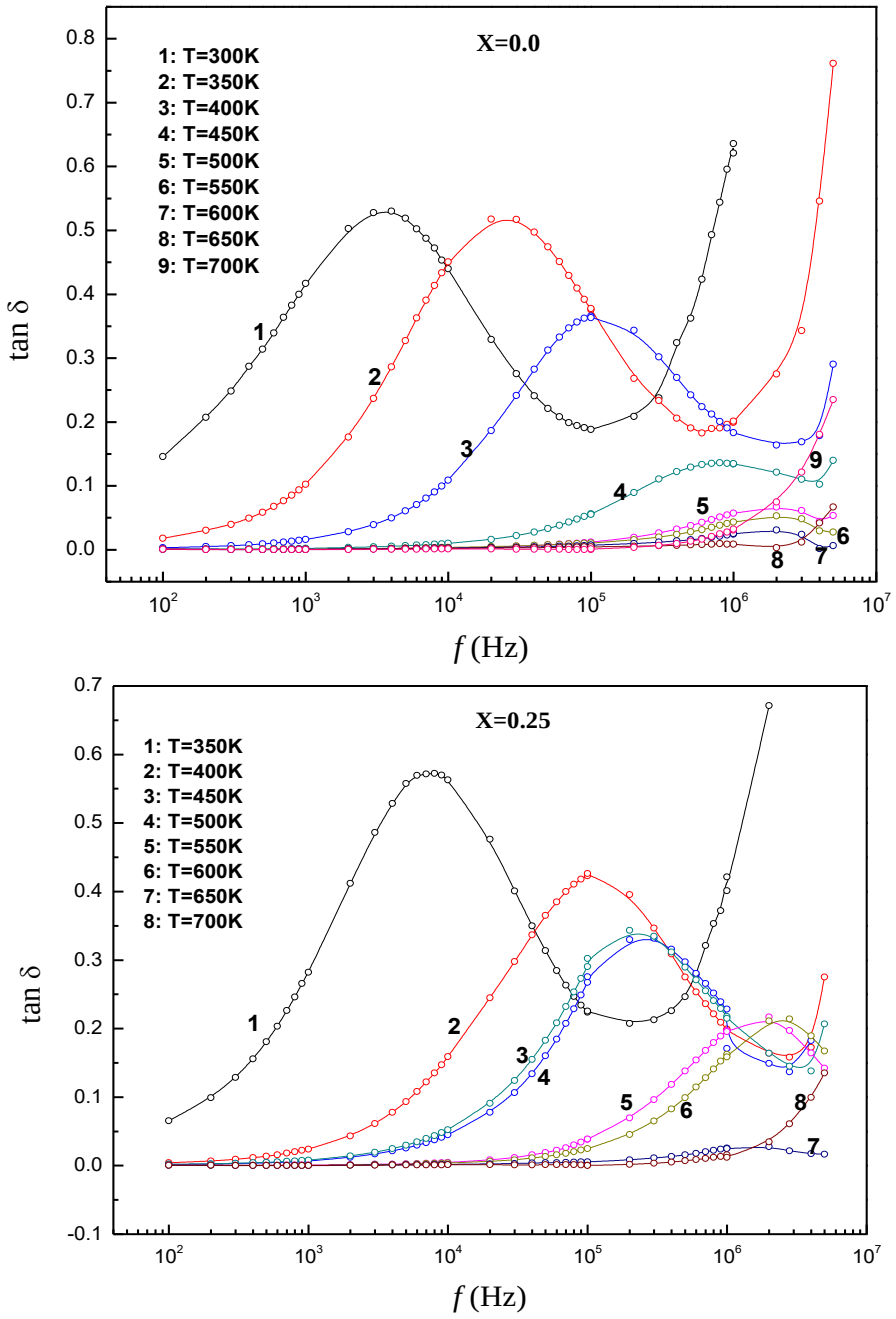

Fig. (3 a : b): The variation of the tanδ with the frequency, *f* (Hz), at different selected temperatures for $Ni_{1-x}Li_{0.5x}Fe_{2+0.5x}O_4$ samples with (x=0.0 & x.=0.25).

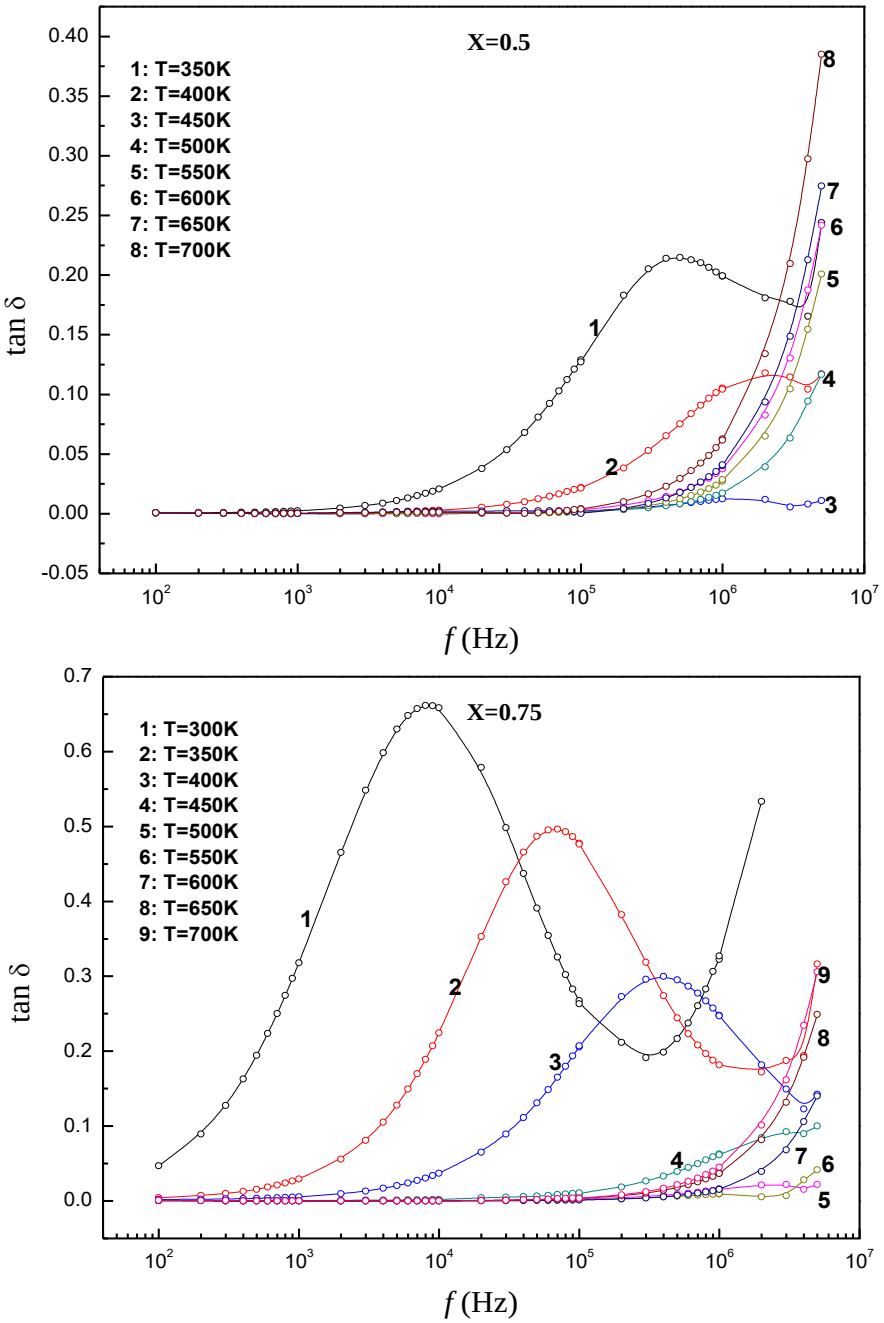

Fig. (3 c : d): The variation of the tanδ with the frequency, *f* (Hz), at different selected temperatures for $Ni_{1-x}Li_{0.5x}Fe_{2+0.5x}O_4$ samples with (x=0.5 & x.=0.75).

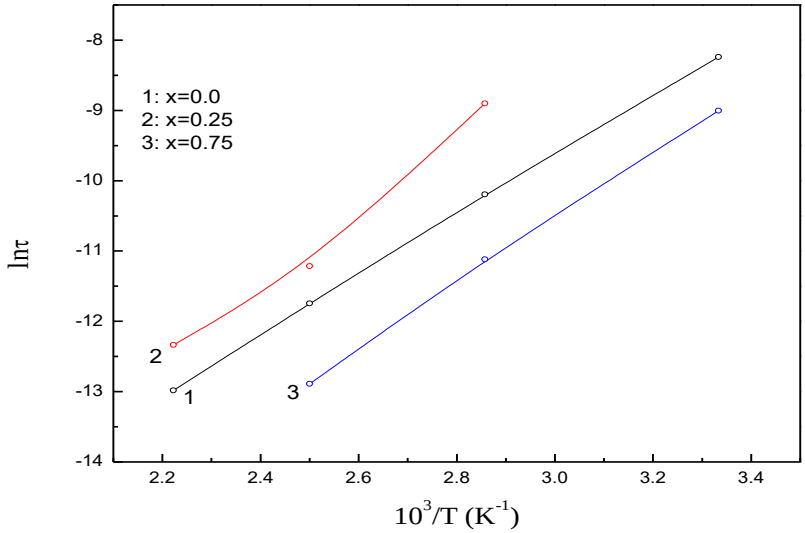

Fig. (4): The variation of lnτ with the temperature (10^3/T) for $Ni_{1-x}Li_{0.5x}Fe_{2+0.5x}O_4$ samples with (x=0.0, x=0.25 & x.=0.75).

Table (1): The dielectric activation energy E_D for $Ni_{1-x}Li_{0.5x}Fe_{2+0.5x}O_4$.

X	0.0	0.25	0.75
E_D (eV)	0.36	0.47	0.4

3.2. AC Electrical Conductivity

AC electrical conductivity, σ′, was measured as a function of both temperature and frequency for $Ni_{1-x}Li_{0.5x}Fe_{2+0.5x}O_4$ (x= 0.0, 0.25, 0.5, and 0.75). The temperature ranges from 300K to 700K, while the frequency ranges from 100 Hz to 5M Hz. Fig. (5) depicts the variation of AC electrical conductivity, as lnσ', with the temperature as 10^3/T, at different selected frequencies (100 Hz, 1 kHz, 10 kHz, 100 kHz, 1 MHz and 5 MHz) for all samples. It is shown that AC electrical conductivity exhibits a semiconducting behavior with the temperature, *i.e.*, the measured AC conductivity, σ′, increases with increasing temperature for all samples. This can be attributed to the increase of the drift mobility (μ) of charge carriers.

Figure (6) shows the variation of the measured AC electrical conductivity, σ′ ($\Omega^{-1}m^{-1}$), with the frequency, *f* (Hz), as log-log scale at different selected temperatures. The results show that σ′ increases with frequency for all samples below nearly 450 K. At temperature higher than 550 K, σ′ seems to be frequency independent. This behavior was reported for

other ferrites [23, 24]. The dispersion of AC electrical conductivity of polycrystalline ferrite can be explained on the basis of Maxwell-Wagner model [25, 26] and Koops phenomenological theory [27], where ferrite is imagined to act as a multiculsters structure in which the ferrite samples are characterized by a microstructure consisting of conductive grains (with conductivity σ_1; dielectric constant ε_1; and diameter d_1) separated by resistive fine grains (with σ_2; ε_2; and d_2). Therefore the highly conductive grains have high values of permittivity, while the fine grains are less conductive with less permittivity. The impedance of such capacitor-like structure can be represented as [28].

$$Z^{-1} = R^{-1} + J\omega C \qquad (7)$$

where ω is the angular frequency ($\omega=2\pi f$), R and C are the parallel equivalent resistance and capacitance of the material, respectively. According to Eq. (7), it is shown that the inverse impedance of the multigrains condenser of ferrite material rises with frequency. On the other hand, as the temperature increases so many clusters sites could be formed through which electron hopping may occur. Depending on the dimensions of the cluster, the electron may hop many times during the effective half period of the external field signal. According to the multiple hopping conduction mechanism, the AC electric conductivity can be written as [29]

$$\sigma'(\omega,T)\ \alpha\ \omega^S T^n$$

where the temperature parameter n depends on the composition and the frequency. The logarithmic representation of this equation is shown in Fig. (7) at the given frequencies 100 Hz, 1kHz, 10 kHz, 100kHz, 1 MHz and 5 MHz. The temperature parameter n was determined from the slopes of the lines and listed in Table (2) at different frequencies. The values of n are always greater than unity and decreases with increasing frequency. The multiple hopping may weakens the frequency dependence but simultaneously may strengthing the temperature dependence, so a multiple hopping mechanism becomes more effective at low frequency and high temperatures. These results are in a good agreement with the previously published results for $BaNi_{2-x}Mg_xFe_{16}O_{27}$ ferrites [23].

Table (2): Variation of the temperature parameter n with the composition at different selected frequencies.

x	n					
	100 Hz	1kHz	10kHz	100kHz	1MHz	5MHz
0.0	11.85	10.94	9.78	8.69	7.9	7.12
0.25	12.07	11.7	11.03	10.36	9.9	9.4
0.5	8.42	8.4	8.399	8.08	7.35	7.09
0.75	11.42	10.97	10.15	9.64	9.24	8.56

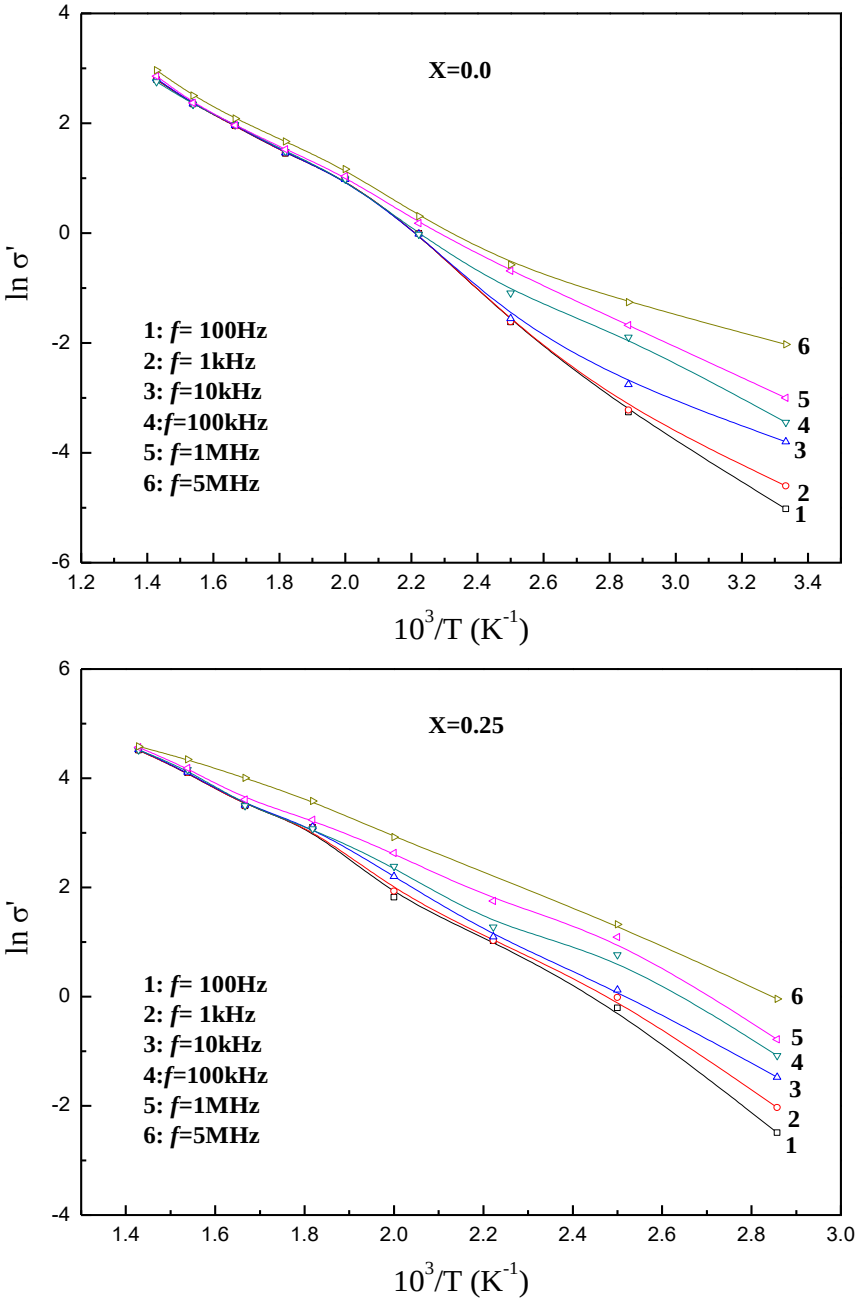

Fig. (5 a – b): The temperature dependence of AC electrical conductivity, σ', at different constant frequencies for $Ni_{1-x}Li_{0.5x}Fe_{2+0.5x}O_4$ samples with (x=0.0 & x.=0.25).

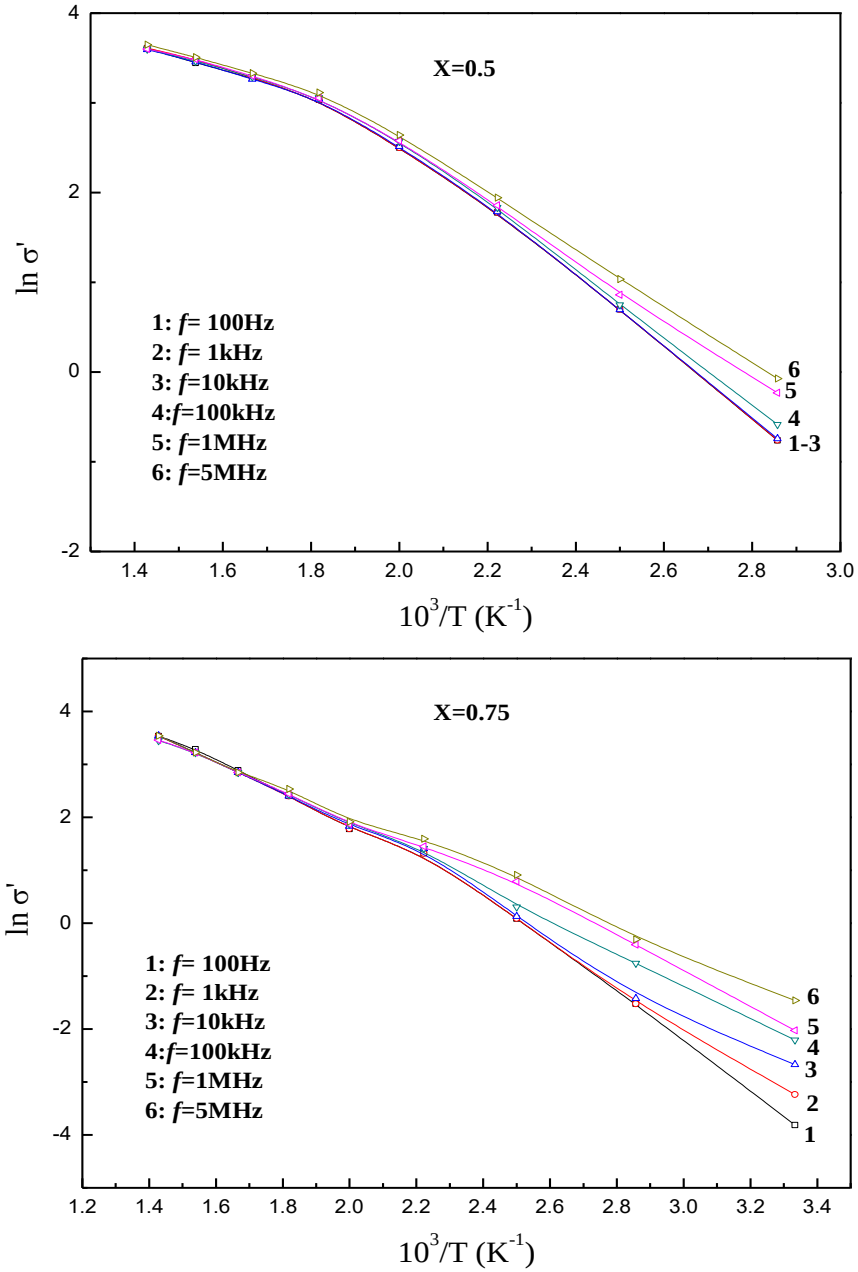

Fig. (5 c – d): The temperature dependence of AC electrical conductivity, σ', at different constant frequencies for $Ni_{1-x}Li_{0.5x}Fe_{2+0.5x}O_4$ samples with (x=0.5 & x.=0.75).

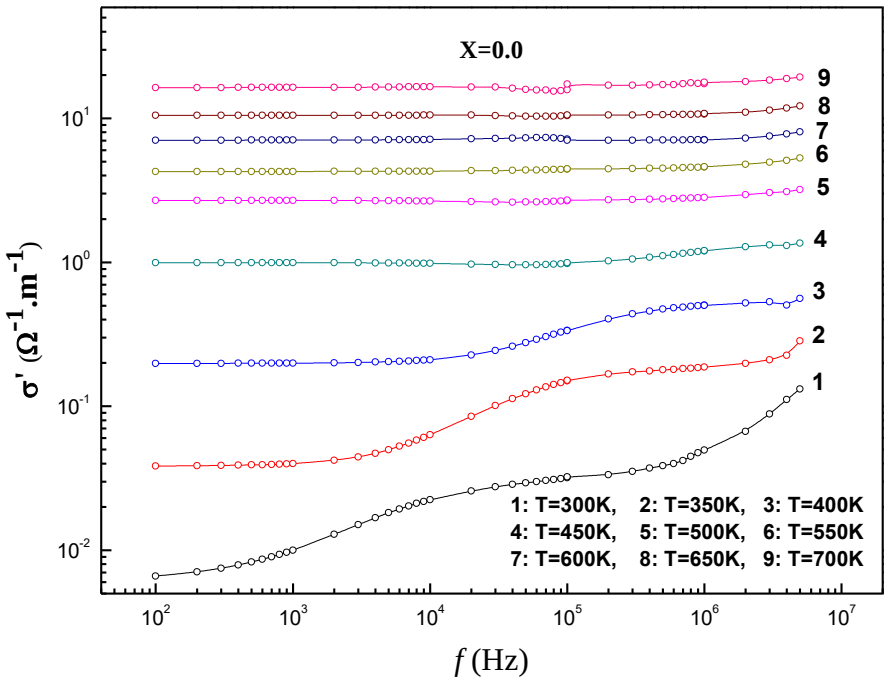

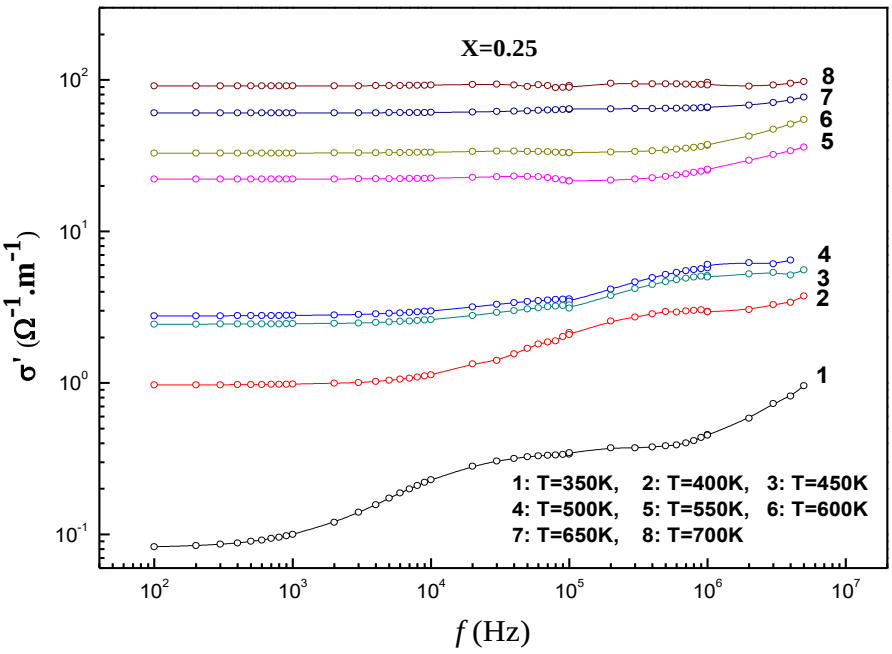

Fig. (6 c – d): AC electrical conductivity as a function of frequency at different constant temperature for $Ni_{1-x}Li_{0.5x}Fe_{2+0.5x}O_4$ samples with (x=0.0 & x.=0.25).

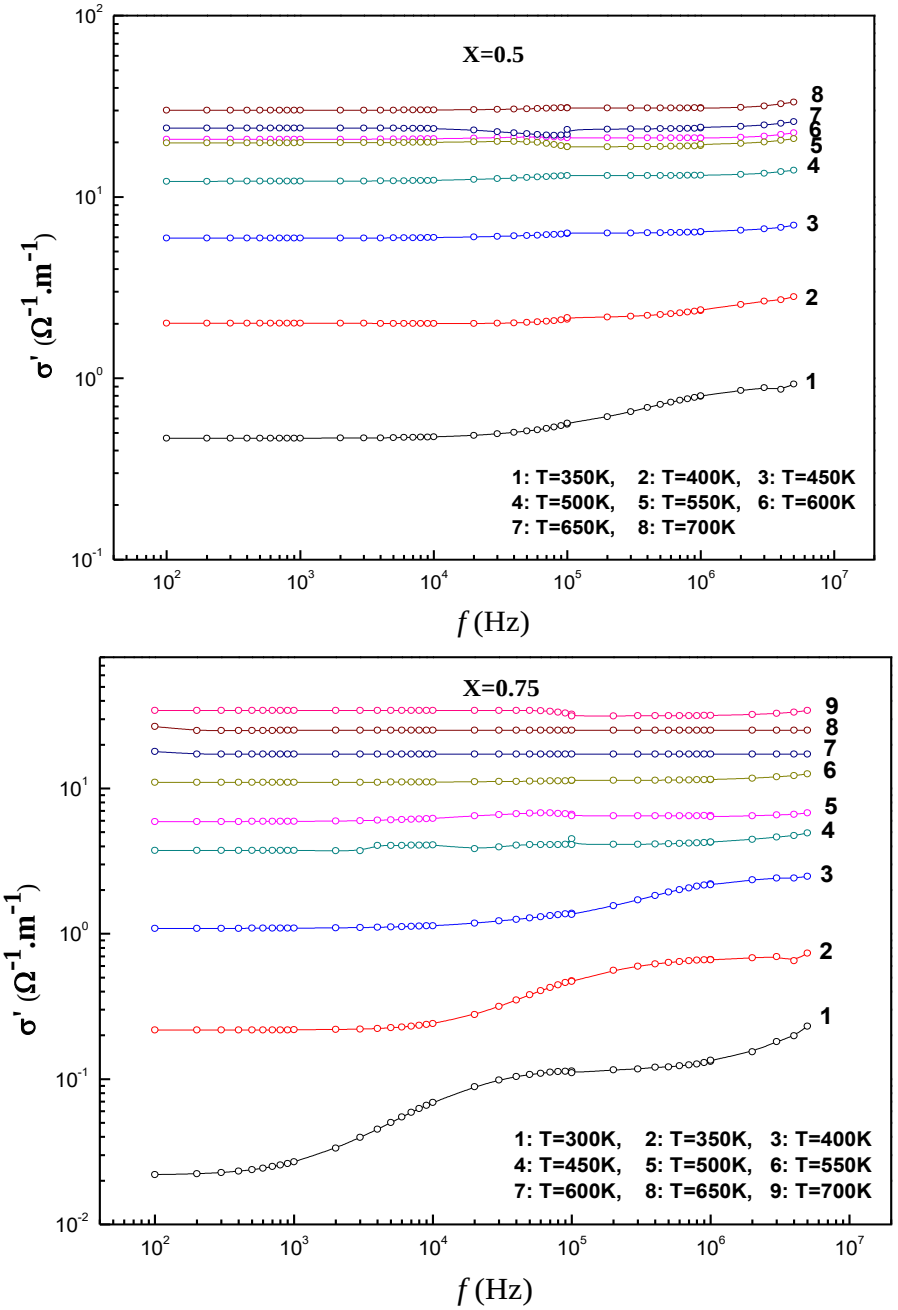

Fig. (6 c – d): AC electrical conductivity as a function of frequency at different constant temperature for $Ni_{1-x}Li_{0.5x}Fe_{2+0.5x}O_4$ samples with (x=0.5 & x.=0.75).

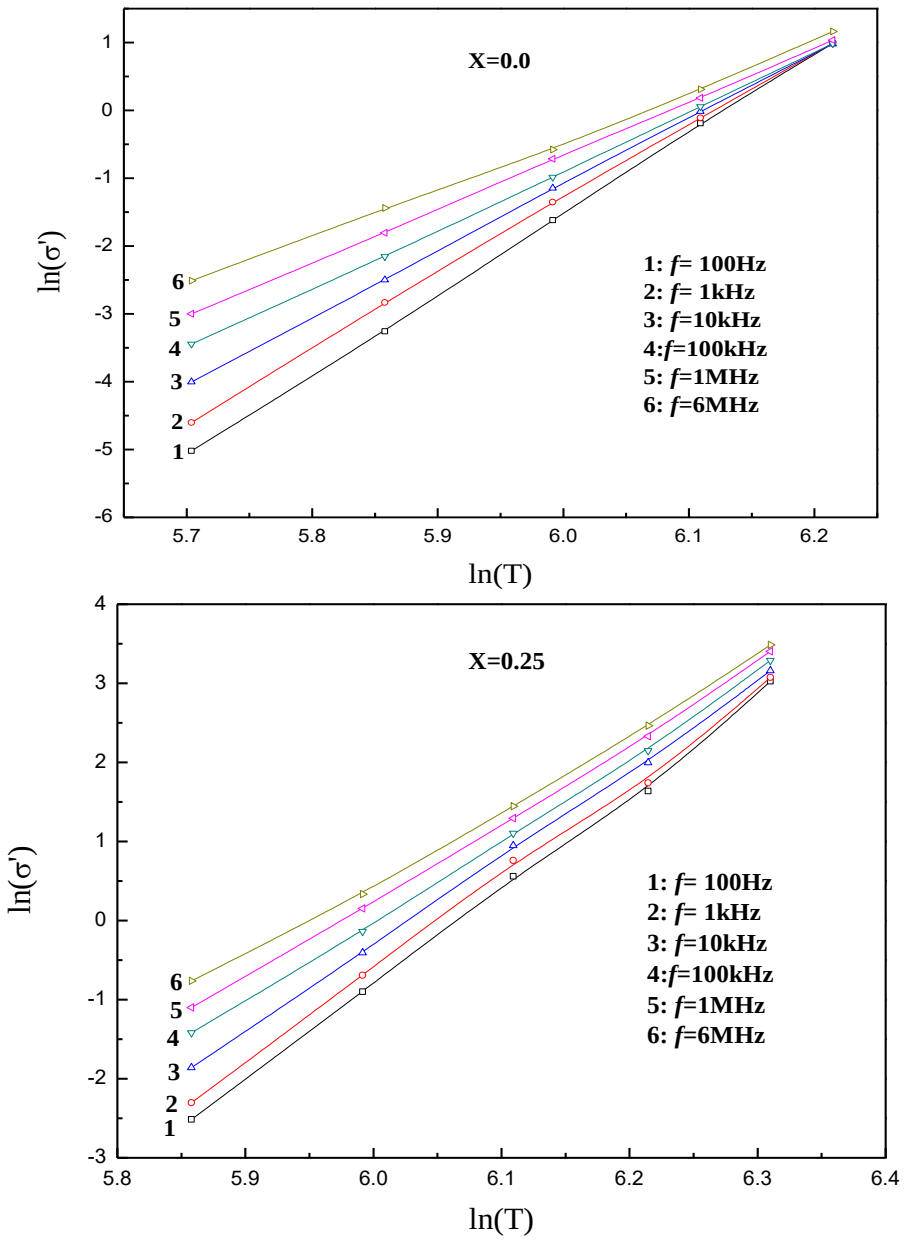

Fig. (7 c – d): Logarithmic representation of the temperature dependence of AC conductivity at different frequencies for $Ni_{1-x}Li_{0.5x}Fe_{2+0.5x}O_4$ samples with (x=0.5 & x.=0.75)..

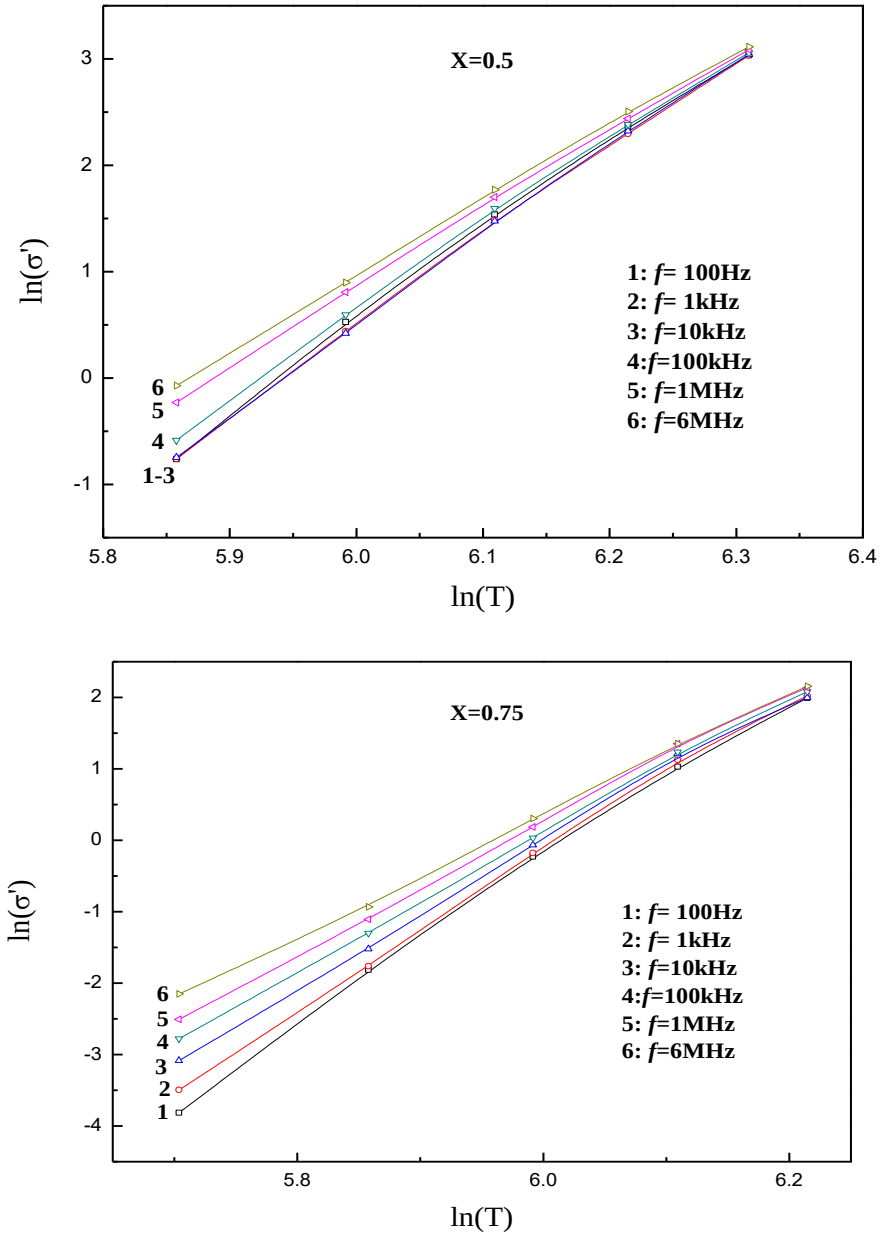

Fig. (7 c – d): Logarithmic representation of the temperature dependence of AC conductivity at different frequencies for $Ni_{1-x}Li_{0.5x}Fe_{2+0.5x}O_4$ samples with (x=0.5 & x.=0.75)..

4. Conclusion

Four samples owing the series $Ni_{1-x}Li_{0.5x}Fe_{2+0.5x}O_4$ were prepared by the ceramic method. AC electrical conductivity and the dielectric constant were measured at different temperatures and frequencies. The results show that, the values of the dielectric constant are abnormally very high ($10^6 - 10^8$) at room temperature. AC electrical conductivity shows semiconducting behavior with the temperature. The multiple hopping conduction mechanism seems to be the most favorable conduction mechanism in these samples.

References

1. T. Murase, K. Igarahi, J. Sawai and T. Nomura, *ICF7*, **B3**, 3 (1996).
2. C. P. Poole and H. A. Farach, *Z. Phys*. B **47**, 55 (1982).
3. D. C. Carter and T. O. Mason, *J. Amer. Ceram. Soc*. **71**, 213 (1988)
4. J. C. Waerenborgh, M. O. Figueiredo, J. M. P. Cabrol, and L. C. J. Pereiro, *J. Solid state chem*. **111**, 300 (1994).
5. B. K. Kuanr, G. P. Srivastava, *J. Appl. Phys*. **75** (10), 6115 (1994).
6. R. Mitra, R. K. Puri, R. G. Mendiratta, *J. Mater. Sci. Lett*. **11**, 276 (1992).
7. M. K. ElNimr, B. M. Moharram, S. A. Saafan, S. T. Assar, *Journal of Magnetism and Magnetic Materials*, **322**, 2108 (2010).
8. P. V. Reddy, T. S. Rao, *J. Less-Common Met*. **79**, 191 (1981).
9. S. A. Mazen, *Phys. Stat. Sol*. (a) **154**, 681 (1996).
10. A. Ahmed, *J. Mater. Sci*. **27**, 4120 (1992).
11. S. A. Mazen, F. Metawe, S. F. Mansour, *J. Phys. D: Appl. Phys*. **30**, 1799 (1997).
12. P. V. Reddy and T. S. Rao, *physica status solidi* (a), 92 (1), 303 (1985).
13. J. Jing, L. Laingchao, X. Feng, and L. Zhiting, *J. of Rare Earths*, **23**, 259 (2005).
14. R. G. Kharabe, R. S. Devan, C. M. Kanamadi, and B. K. Chougule, *Smart Materials and Structures*, **15**(2), N36 (2006).
15. K. M. Batoo, S. Kumar, C. G. Lee, Alimuddin, *Current Applied Physics*, **9**, 826 (2009).
16. W. D. Kingery, H.K. Bouen, D. R. Ublmanm, in: "*Introduction to Ceramics*", 2nd Edition, Wiley, New York, (1976).
17. V. R. K. Murthy, J. Sobhamadri, *Phys. Status Solidi*, A **36**, 133 (1976).
18. N. Rezlescu, E. Rezlescu, *Phys. Status Solidi* A **59**, 323 (1980).
19. K. Iwauchi, *J. Appl. Phys*. **10**, 1520 (1971).
20. M. M. El-Desoky and I. Kashif, *Phys. Stat. Sol*., **194**, No. 1, 89 (2002).
21. M. B. Reddy, P. V. Reddy, Phys. D: *Appl. Phys*. **24**, 975 (1991).
22. K. Standly, *Oxide Magnetic Materials*, Clarendon Press, Oxford, 114 (1974).

23. S. M. Attia, A. M. Abo El Ata, D. El Kony, *JMMM*, **270**, 142 (2004).
24. A. M. Abo El Ata, S. M. Attia, T. M. Meaz, *Solid State Sciences*, **6**, 61 (2004).
25. J. C. Maxwell, *Electricity and Magnetism*, vol. 1, Oxford University Press, 328 (1873).
26. K. Wagner, *Ann. Phys*. **40**, 817 (1913).
27. C. G. Koops, *Phys. Rev*. **83** (1), 121 (1951).
28. S. A. Mazen, H.M. Zaki, *J. Phys. D: Appl. Phys*. **28**, 1 (1995).
29. S. Abboudy, M. A. Ahmed, A. M. Abo El Ata, *Phys. Low-Dim. Struct*., **5/6**, 107 (2001).